Journal of Applied Toxicology

WILEY

Journal of AppliedToxicology

RESEARCH ARTICLE

Monosodium Glutamate Exposure and Liver Damage: Modulatory Effects of L-Carnitine on Inflammation and Autophagy

Kubra Tuğce Kalkan[1] | Ferhat Pektas[2]

[1]Department of Histology and Embryology, Faculty of Medicine, Kırsehir Ahi Evran University, Kırşehir, Turkey | [2]Department of Physiology, Faculty of Medicine, Kırsehir Ahi Evran University, Kırşehir, Turkey

Correspondence: Kubra Tuğce Kalkan (ktugce.kalkan@gmail.com)

Received: 21 September 2025 | **Revised:** 4 November 2025 | **Accepted:** 19 November 2025

Keywords: autophagy | inflammation | L-carnitine | liver | monosodium glutamate

ABSTRACT

Monosodium glutamate (MSG), a widely used flavor enhancer, has been associated with hepatotoxicity through mechanisms involving oxidative stress, inflammatory activation, and disruption of autophagy. L-Carnitine, recognized for its antioxidant and anti-inflammatory effects, has been proposed as a potential therapeutic agent against liver injury. This study aimed to evaluate the hepatotoxic effects of monosodium glutamate (MSG) and the therapeutic potential of L-carnitine in mitigating MSG-induced liver injury, with emphasis on autophagy-related pathways. Forty male offspring obtained from 12 pregnant Wistar albino rats were divided into five groups ($n = 8$ per group): control, sham, MSG, L-carnitine, and MSG + L-carnitine. Neonatal rats received MSG (4 g/kg, s.c.) on postnatal days 2, 4, 6, 8, and 10, whereas L-carnitine (200 mg/kg, i.p.) was administered between postnatal days 60–81. Biochemical, histopathological, and immunohistochemical analyses were performed. MSG exposure significantly increased serum ALT levels ($p < 0.05$) and caused marked histological alterations, including cytoplasmic vacuolization ($p < 0.001$), eosinophilia ($p < 0.001$), sinusoidal dilatation ($p < 0.001$), and fibrosis ($p < 0.001$). [Correction added on 13 January 2026, after first online publication: The phrase "AST (p<0.001) and ALT (p<0.001) levels" has been revised to "ALT levels (p<0.05)" in the previous sentence.] Immunohistochemically, MSG reduced mTOR immunoreactivity by 4% ($p < 0.05$) while increasing ULK1 by 6% ($p < 0.01$) and ATG13 by 3.5% ($p < 0.05$). L-Carnitine treatment significantly decreased histological damage scores (vacuolization −28%, fibrosis −25%, all $p < 0.05$), restored mTOR levels ($p > 0.05$ vs. control), and attenuated ULK1 and ATG13 overexpression ($p < 0.01$). These findings demonstrate that L-carnitine exerts a therapeutic effect against MSG-induced hepatocellular injury by modulating oxidative stress, inflammatory cytokines, and autophagy imbalance via the mTOR–ULK1–ATG13 pathway.

1 | Introduction

Monosodium glutamate (MSG), the sodium salt of glutamate, is widely used as a flavor enhancer, especially in processed and packaged foods (Oluwole et al. 2024). Due to rapid urbanization, industrialization, and increasingly busy work schedules, the consumption of ready-to-eat foods has increased, leading to greater use of additives such as MSG (Adeleke et al. 2022). Recent studies on animals and cell cultures have shown that MSG can exert toxic effects from early development through adulthood, associated with oxidative stress, mitochondrial dysfunction, inflammation, and apoptosis. As a result, MSG exposure has been linked to various systemic complications, including cardiovascular diseases, hepatotoxicity, central nervous system injury, gastrointestinal disorders, hormonal imbalance, sexual dysfunction, and obesity (Bayram et al. 2023). The liver, as the central organ of metabolism, is particularly vulnerable to the harmful effects of MSG (Zanfirescu et al. 2019). MSG decreases antioxidants such as GSH, SOD, and CAT, elevates MDA levels, enhances oxidative stress in the liver, and induces

cellular injury through lipid peroxidation. Histopathological studies have revealed MSG-induced hepatic alterations such as hepatocellular vacuolation, degeneration, nuclear pyknosis, and cytoplasmic loss. In addition, congestion in centrilobular veins, sinusoidal obstruction, and, in some cases, inflammatory infiltration and fibrotic band formation in the portal region have been reported (Kasmara et al. 2025).

Previous studies have demonstrated that MSG upregulates the expression of proinflammatory cytokines such as interleukin-6 (IL-6) and tumor necrosis factor-alpha (TNF-α) (Eid et al. 2019; Banerjee et al. 2021; Asejeje et al. 2023). MSG has also been reported to increase cellular damage by suppressing the autophagy process (Morsy et al. 2025). Autophagy is an essential cellular mechanism that degrades and recycles damaged organelles and proteins through the lysosomal pathway to maintain homeostasis under stress (Lim et al. 2024). This process is regulated by several signaling pathways, with mTOR, ULK1, and Atg13 serving as key molecular components. The regulatory kinase mTOR senses the cell's nutrient and energy status and inhibits autophagy. ULK1, a serine–threonine kinase, initiates autophagy, but its activity is inhibited when mTOR is activated. Atg13 interacts with ULK1 to form a complex that stabilizes the autophagy machinery and plays a crucial role in its initiation (Ganley et al. 2009). Key proinflammatory cytokines such as TNF-α and IL-1β trigger inflammatory responses when cells are damaged, infected, or exposed to stress. Autophagy and inflammation are interconnected through bidirectional interactions between TNF-α and IL-1β, whose levels can fluctuate dynamically during this process (García-Miguel et al. 2018; Sun et al. 2017).

L-Carnitine is a naturally occurring compound in all mammals that transports long-chain fatty acids into mitochondria for β-oxidation. It is mainly obtained from dietary sources such as meat and dairy products and is also synthesized in the liver and kidneys from the amino acids L-lysine and L-methionine (Virmani and Cirulli 2022). L-Carnitine plays an essential role in metabolism and reduces oxidative stress, thereby supporting tissue repair (Ribas et al. 2014). It strengthens the antioxidant defense system, offering preventive and therapeutic benefits, particularly in metabolically active organs such as the liver. Administration of L-carnitine has been shown to reduce necrotic areas, inflammation, and hepatocyte degeneration in liver tissue (Alqhtani 2025). Based on this evidence, the present study investigates the adverse effects of MSG on liver tissue and evaluates the potential therapeutic role of L-carnitine using histological, immunohistochemical, and biochemical analyses. Importantly, although the toxic effects of MSG and the therapeutic role of L-carnitine have been explored in different tissues, no previous study has comprehensively addressed their relationship in liver tissue with a specific focus on autophagy-related markers such as mTOR, ULK1, and Atg13. Therefore, our research aims to fill this critical gap by elucidating the interplay between MSG-induced liver injury, autophagy dysregulation, and the modulatory potential of L-carnitine. We hypothesize that L-carnitine exerts hepatorestorative effects against MSG-induced toxicity by attenuating oxidative stress and inflammation and by regulating autophagy-related pathways involving mTOR, ULK1, and Atg13.

2 | Materials and Methods

2.1 | Ethical Acceptance

The Kırşehir Ahi Evran University Animal Experiments Local Ethics Committee examined this study and accepted our experimental procedures (decision no: 11/02, date: 27.05.2025). All procedures involving animals were carried out in accordance with international guidelines for the care and use of laboratory animals, and every effort was made to minimize animal suffering. The study design and reporting also adhered to the ARRIVE (Animal Research: Reporting of In Vivo Experiments) guidelines to ensure methodological transparency and reproducibility.

2.2 | Study Design and Animals

A total of 40 male offspring rats were generated from 12 pregnant Wistar albino females obtained from the Experimental Animals Facility of Kırşehir Ahi Evran University. Prior to experimentation, breeders were allowed a 1-week adaptation period under laboratory conditions. Mating was performed at a ratio of two females to one male per cage, and the appearance of a vaginal plug was accepted as gestational day 0 (GD0). After confirmation of pregnancy, the females were maintained in groups of three per standard cage. When delivery was imminent, each dam was relocated to an individual cage to enable precise observation. During the entire study, animals were kept under stable conditions: 22°C°C ± 2°C temperature, 50% ± 5% relative humidity, and a 12-h light/dark cycle (lights on at 07:00). Standard pellet chow and tap water were provided ad libitum. The feed consisted of 23.5% crude protein, 3.15% crude fat, 4.91% crude ash, 4.96% crude fiber, and 3.13% mineral additives. All animals delivered without intervention, and both the total number of offspring and their individual birth weights were registered.

2.3 | Experimental Groups

Newborn rats in the MSG group received subcutaneous (s.c.) injections of monosodium glutamate (MSG) at a dose of 4 g/kg body weight, dissolved in normal saline, on alternate days, specifically postnatal days (PND) 2, 4, 6, 8, and 10. The neonatal rats weighed approximately 8–10 g at birth. MSG was administered on postnatal days 2, 4, 6, 8, and 10, corresponding to a total of five injections given at 1-day intervals starting from Day 2 after birth. At the end of the fifth injection, the neonates were 10 days old. In comparison, newborns in the sham group received 0.9% saline subcutaneous injections at a volume of 0.1 mL/g on the same PND. The newborns stayed with their mothers until weaning day, PND21, when the rats were housed in groups of four in separate cages and fed daily. On days PN60-81, rats in the L-carnitine and MSG + L-carnitine groups were administered 200 mg/kg of L-carnitine. Rats were randomly assigned into five groups, as follows: control group (healthy group), sham group (given 0.1 mL saline), and MSG group (given 4 g/kg MSG [s.c.]) (Kayode et al. 2023). L-Carnitine group (provided L-carnitine 200 mg/kg PND60-81) (Koohpeyma et al. 2022), MSG + L-carnitine group (given MSG [s.c.] 4 g/kg, PND 2-10

and L-carnitine 200 mg/kg PND 60-81). MSG (monosodium glutamate, Sigma, Almanya; CAS #: 6106-04-3) and L-carnitine (L-carnitine, Sigma, Almanya; CAS #: 541-15-1) were obtained from Sigma.

2.4 | Histopathological Assessment

For histological analysis of the differences in liver tissue in each experimental group, tissue samples collected at the conclusion of the studies were preserved in a 10% formaldehyde solution. The tissues had been in contact with formaldehyde for 72 h before being washed under running water. After several phases of alcohol dehydrations, they were purified in xylene, embedded in paraffin, and paraffin blocks were formed. Rat liver paraffin blocks were cut into 5-μm-thick sections and placed on slides. The sections were stained with hematoxylin and eosin (H&E) and Masson's trichrome (MT). Following staining, sections were exposed to ascending alcohol passes, xylene clearing, coverslip mounting, and light microscopy analysis (Nikon Eclipse Si, Tokyo, Japan). In addition, liver tissue damage was evaluated for cytoplasmic vacuolization, cytoplasmic eosinophilia, and sinusoidal dilatation and rated. This assessment was graded semiquantitatively on a scale of 0–3 for each criterion (0 = *none*, 1 = *mild*, 2 = *moderate*, 3 = *severe*).

2.5 | Immunohistochemical Evaluation

Immunohistochemistry indicated the expression of TNF-α, IL-1β, mTOR, ULK1, and Atg13 in liver tissue. The avidin-biotin peroxidase assay was used in immunohistochemical staining. To stain, 5 μm slices of paraffin blocks were cut on polylysine slides. Sections were deparaffinized with xylol and then preserved with a decreasing alcohol before being dehydrated in distilled water. Sections were cooked in a 600-W microwave oven with 5% citrate buffer for antigen retrieval, washed with phosphate-buffered saline (PBS), and treated with 3% H_2O_2 to inhibit endogenous peroxidase activity. All subsequent stages used the immunohistochemical staining kit (Thermo Scientific/TS-125-HR, Thermo Fisher Scientific Inc., Waltham, MA, USA), and the treatment was carried out in a setting that prevents tissue drying. To cover the areas outside of the antigenic regions, block serum was injected into PBS-washed sections and allowed to rest at room temperature for 10 min. After that, the primary antibodies for TNF-α (Elabscience, e-ab-68252, 1:100), IL-1β (Proteintech, 26048-1-ap, 1:200), mTOR (Proteintech, Cat No. 66888-1-Ig, 1/1000), ULK1 (Proteintech, Cat No. 20986-1-AP, 1:100), and ATG13 (Proteintech; Cat No. 18258-1-AP, 1:250) were incubated for a full night at 4°C. The sections were then incubated via biotinylated secondary antibodies. After PBS washing, the streptavidin–peroxidase mix was applied. The sections were then washed and treated with diaminobenzidine (DAB) (diaminobenzidinechromogen and substrate system, 125 mL from Thermo Fisher Scientific, Waltham, Massachusetts, USA) substrate to make immunoreactivities visible, followed by a 5-min wash with distilled H_2O. The tissues were then placed in a sequence of increasing alcohols, xylene, and entellan that avoided air bubble formation. The sections where the immunohistochemical staining procedure was used were inspected under a light microscope, and microscopic photos were taken from 10 separate areas. The immunoreactivity of the markers observed in the histological images was quantified using ImageJ software by applying a standardized color threshold method to assess staining intensity, and the results were recorded.

2.6 | AST and ALT Level Measurement

The collected blood samples were placed in biochemical tubes, allowed to stand upright for 40 min, and then centrifuged at 3000 rpm for 10 min to separate the serum. After centrifugation, the obtained serum samples were stored at −80°C until biochemical analysis. Serum aspartate aminotransferase (AST; Otto Scientific, Cat. No: OttoBC127) and alanine aminotransferase (ALT; Otto Scientific, Cat. No: OttoBC128) levels were analyzed colorimetrically using an automated biochemical analyzer (Mindray BS400, Shenzhen, China) in accordance with the manufacturer's instructions.

2.7 | Statistical Analysis

GraphPad Prism Version 9 was used for all statistical study. The Shapiro–Wilk test was used to check the data distribution. For evaluations involving more than two groups, one-way analysis of variance (ANOVA) and the Kruskal–Wallis test were employed. The Dunn test for the Kruskal–Wallis analysis and the Bonferroni test for the one-way ANOVA were used to identify significant post hoc comparisons of the variables. A significance level of less than 0.05 was considered statistically significant for all data.

3 | Results

3.1 | Liver Histopathology Assessment

Liver histology was evaluated in all groups using H&E staining, and Figure 1A presents representative micrographs at two magnifications (200× and 400×). In the control group, hepatocytes were arranged in regular cords radiating from the central vein, and the sinusoidal spaces were clearly visible, indicating preserved normal hepatic architecture. The overall morphology of the sham group was comparable to that of the control group. Similarly, the L-carnitine group exhibited a hepatic structure consistent with normal histological features.

In contrast, the MSG group showed marked disruption of the hepatic cord organization and loss of the typical lobular structure. Hepatocytes displayed evident vacuolization and increased cytoplasmic eosinophilia, along with sinusoidal dilatation. Compared with the control ($p < 0.001$), sham ($p < 0.001$), and L-carnitine ($p < 0.01$) groups, cytoplasmic vacuolization was significantly increased in the MSG group. Treatment with L-carnitine significantly reduced this score in the MSG + L-carnitine group compared with the MSG group ($p < 0.05$). Cytoplasmic eosinophilia was significantly higher in the MSG group compared to the control ($p < 0.001$), sham ($p < 0.001$), and L-carnitine ($p < 0.001$) groups, whereas L-carnitine administration significantly decreased this parameter compared to the MSG group ($p < 0.001$). Similarly, sinusoidal dilatation was

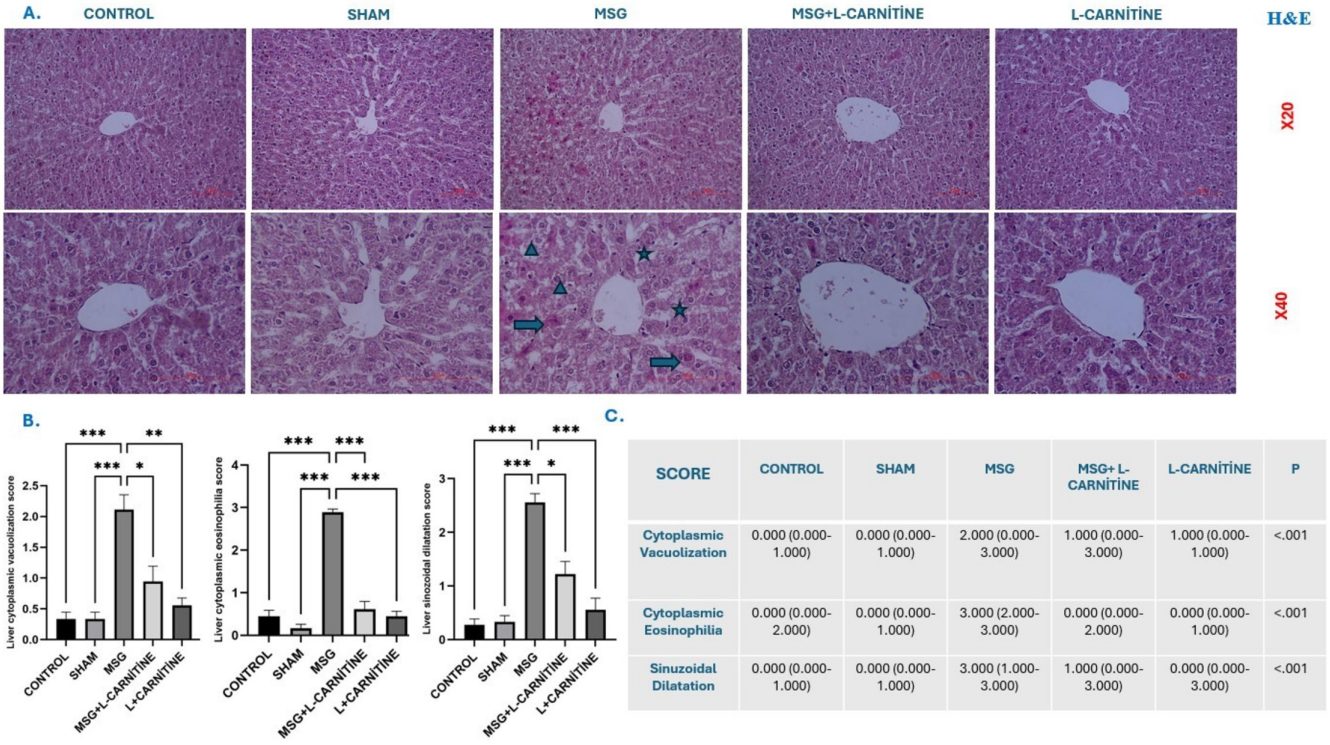

SCORE	CONTROL	SHAM	MSG	MSG+ L-CARNİTİNE	L-CARNİTİNE	P
Cytoplasmic Vacuolization	0.000 (0.000-1.000)	0.000 (0.000-1.000)	2.000 (0.000-3.000)	1.000 (0.000-3.000)	1.000 (0.000-1.000)	<.001
Cytoplasmic Eosinophilia	0.000 (0.000-2.000)	0.000 (0.000-1.000)	3.000 (2.000-3.000)	0.000 (0.000-2.000)	0.000 (0.000-1.000)	<.001
Sinuzoidal Dilatation	0.000 (0.000-1.000)	0.000 (0.000-1.000)	3.000 (1.000-3.000)	1.000 (0.000-3.000)	0.000 (0.000-3.000)	<.001

FIGURE 1 | (A) Light microscopic findings in rat liver tissue. (Nikon Eclipse Si, Tokyo, Japan, 200× and 400×). The MSG group of HE-stained histological section is shown as cytoplasmic vacuolization (blue triangle), cytoplasmic eosinophilia (blue arrow), and sinusoidal dilatation (blue star). (B) Graphical representation of cytoplasmic vacuolization, cytoplasmic eosinophilia, and sinusoidal dilatation in rat liver tissue groups. *$p<0.05$, **$p<0.01$, ***$p<0.001$. Values are represented as mean ± SD using ANOVA and Kruskal–Wallis, followed as a post hoc Tukey test and Dunn's test, respectively. (C) Presentation of histopathological scores of liver tissue in different experimental groups in table form. Data were presented as mean ± standard deviation and median (min–max).

significantly elevated in the MSG group relative to the control ($p<0.001$), sham ($p<0.001$), and L-carnitine ($p<0.001$) groups, and this alteration was markedly attenuated by L-carnitine treatment ($p<0.05$) (Figure 1B,C).

Collagen deposition was evaluated using MT staining. In the MSG group, increased perivascular collagen accumulation and connective tissue deposition were observed (Figure 2A). This increase was statistically significant compared with the control ($p<0.001$), sham ($p<0.001$), and L-carnitine ($p<0.001$) groups. Although the perivascular fibrosis score in the MSG + L-carnitine group was lower than in the MSG group, the difference was not statistically significant ($p>0.05$) (Figure 2B,C).

3.2 | Immunohistochemical Evaluation of Proinflammatory Markers

TNF-α and IL-1β, as proinflammatory markers, were detected in liver tissue using immunohistochemistry. Immunoreactivity, indicated by brown DAB staining in Figure 3A, was compared among the experimental groups. The control, sham, and L-carnitine groups showed low levels of TNF-α immunoreactivity, primarily limited to scattered hepatocytes. In contrast, the MSG group exhibited markedly increased staining intensity, especially in hepatocytes surrounding the central vein and along the sinusoidal borders. The TNF-α immunoreactivity index was significantly higher in the MSG group compared with the control group ($p<0.01$), sham group ($p<0.001$), and L-carnitine group ($p<0.01$). Administration of L-carnitine significantly attenuated this increase in the MSG + L-carnitine group ($p<0.001$) (Figure 3B,C).

The control, sham, and L-carnitine groups demonstrated weak IL-1β immunoreactivity in the portal area and hepatocytes. The MSG group showed intense and widespread IL-1β staining, particularly in the central vein, portal region, bile ducts, and periportal hepatocytes (Figure 3A). The IL-1β immunoreactivity index was significantly elevated in the MSG group compared with the control ($p<0.001$) and sham ($p<0.001$) groups. Treatment with L-carnitine significantly reduced this index in the MSG + L-carnitine group ($p<0.01$) (Figure 3B,C).

3.3 | Immunohistochemical Evaluation of Autophagy Markers

The immunoreactivity indices of autophagy-related markers mTOR, ULK1, and ATG13 were evaluated and compared among the experimental groups. Immunoreactivity, indicated by brown DAB staining, is illustrated in Figure 4A. In the control and sham groups, hepatocytes exhibited extensive and intense cytoplasmic staining, reflecting high mTOR immunoreactivity. Similarly, the L-carnitine group showed a staining

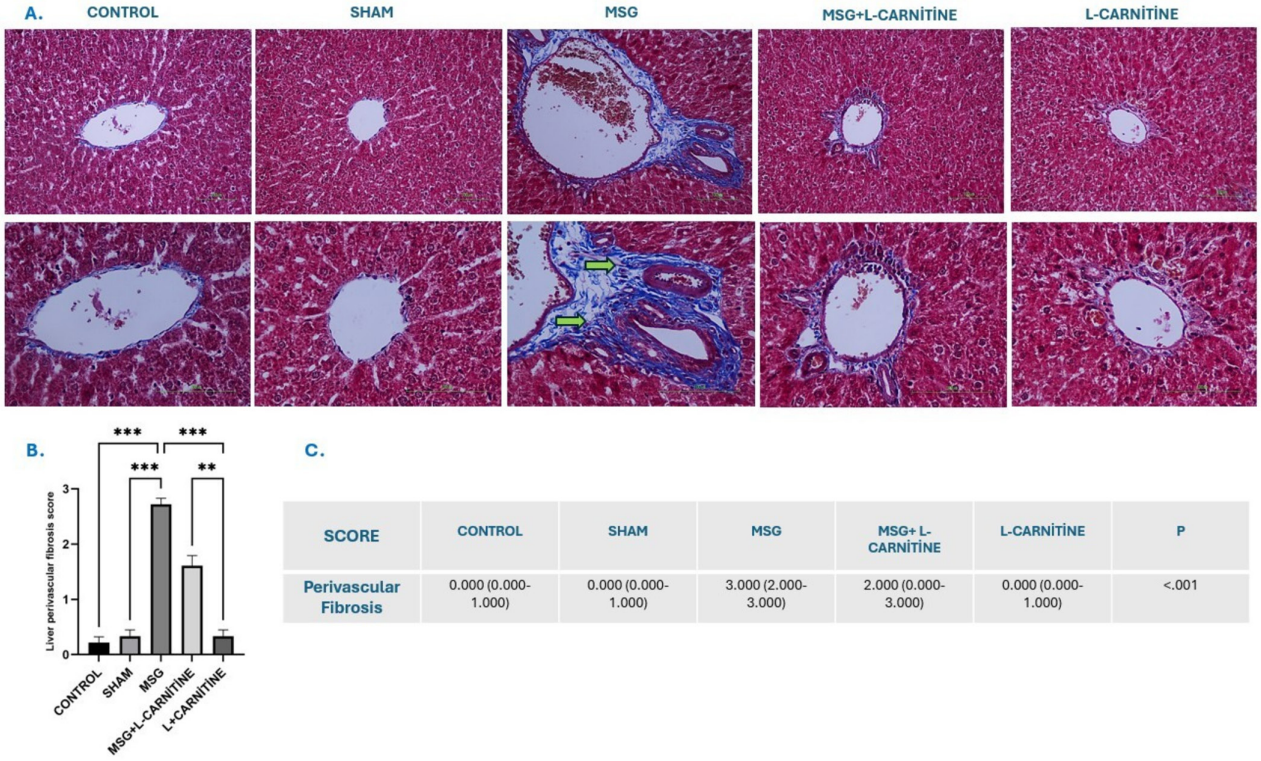

SCORE	CONTROL	SHAM	MSG	MSG+ L-CARNİTİNE	L-CARNİTİNE	P
Perivascular Fibrosis	0.000 (0.000-1.000)	0.000 (0.000-1.000)	3.000 (2.000-3.000)	2.000 (0.000-3.000)	0.000 (0.000-1.000)	<.001

FIGURE 2 | (A) Light microscopic findings in rat liver tissue. (Nikon Eclipse Si, Tokyo, Japan, 200× and 400×). The MSG group of MT stained histological section is shown as perivascular fibrosis (green arrow). [Correction added on 13 January 2026, after first online publication: The "IBU" group has been corrected to the "MSG" group in this version.] (B) Graphical representation of perivascular fibrosis in rat liver tissue groups. *$p < 0.05$, **$p < 0.01$, ***$p < 0.001$. Values are represented as mean ± SD using ANOVA and Kruskal–Wallis, followed as a post hoc Tukey test and Dunn's test, respectively. (C) Presentation of fibrosis scores of liver tissue in different experimental groups in table form. Data were presented as mean ± standard deviation and median (min–max).

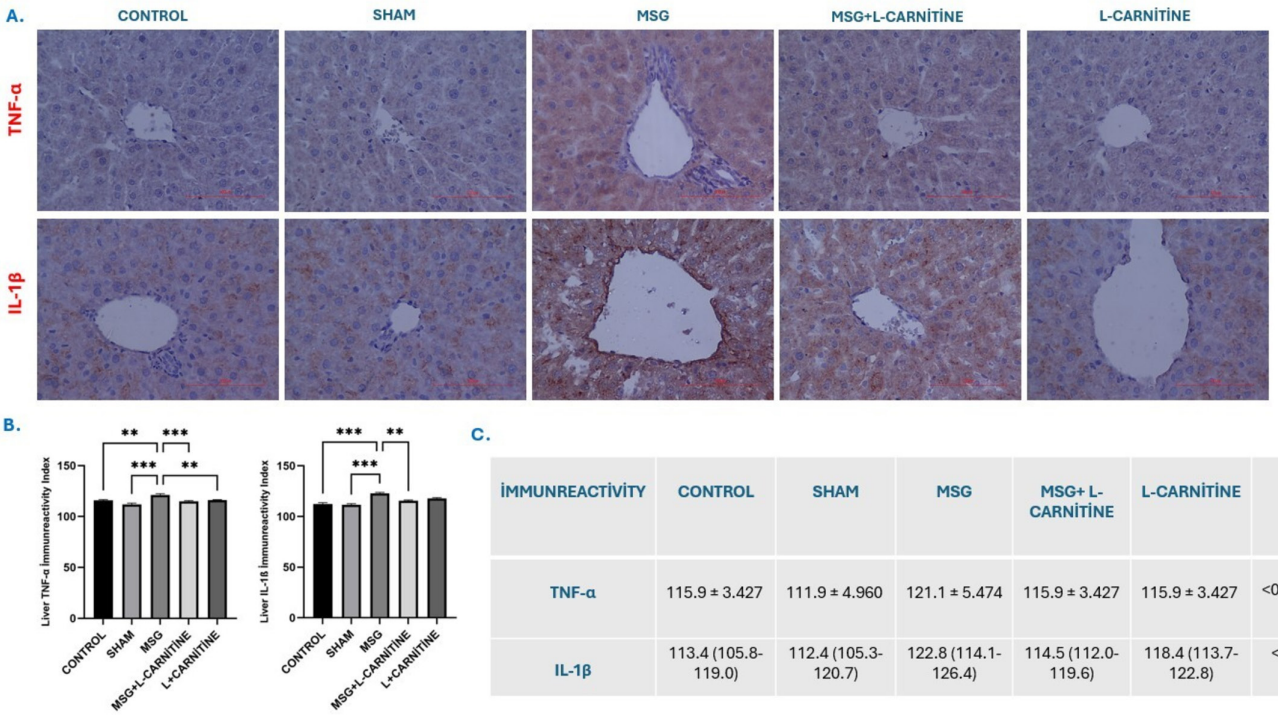

İMMUNREACTİVİTY	CONTROL	SHAM	MSG	MSG+ L-CARNİTİNE	L-CARNİTİNE	P
TNF-α	115.9 ± 3.427	111.9 ± 4.960	121.1 ± 5.474	115.9 ± 3.427	115.9 ± 3.427	<0.0001
IL-1β	113.4 (105.8-119.0)	112.4 (105.3-120.7)	122.8 (114.1-126.4)	114.5 (112.0-119.6)	118.4 (113.7-122.8)	<.001

FIGURE 3 | (A) Immunohistochemical light microscopic findings of TNF-α and IL-β immunoreactivity in rat liver tissue of all groups. (Nikon Eclipse Si, Tokyo, Japan, 400×). Brown colored areas with DAB indicate positivity. (B) Graphical representation of TNF-α and IL-β immunoreactivity in rat liver tissue groups. *$p < 0.05$, **$p < 0.01$, ***$p < 0.001$. Values are represented as mean ± SD using ANOVA and Kruskal–Wallis, followed as a post hoc Tukey test and Dunn's test, respectively. (C) Presentation of TNF-α and IL-β immunoreactivity of liver tissue in different experimental groups in table form. Data were presented as mean ± standard deviation and median (min–max).

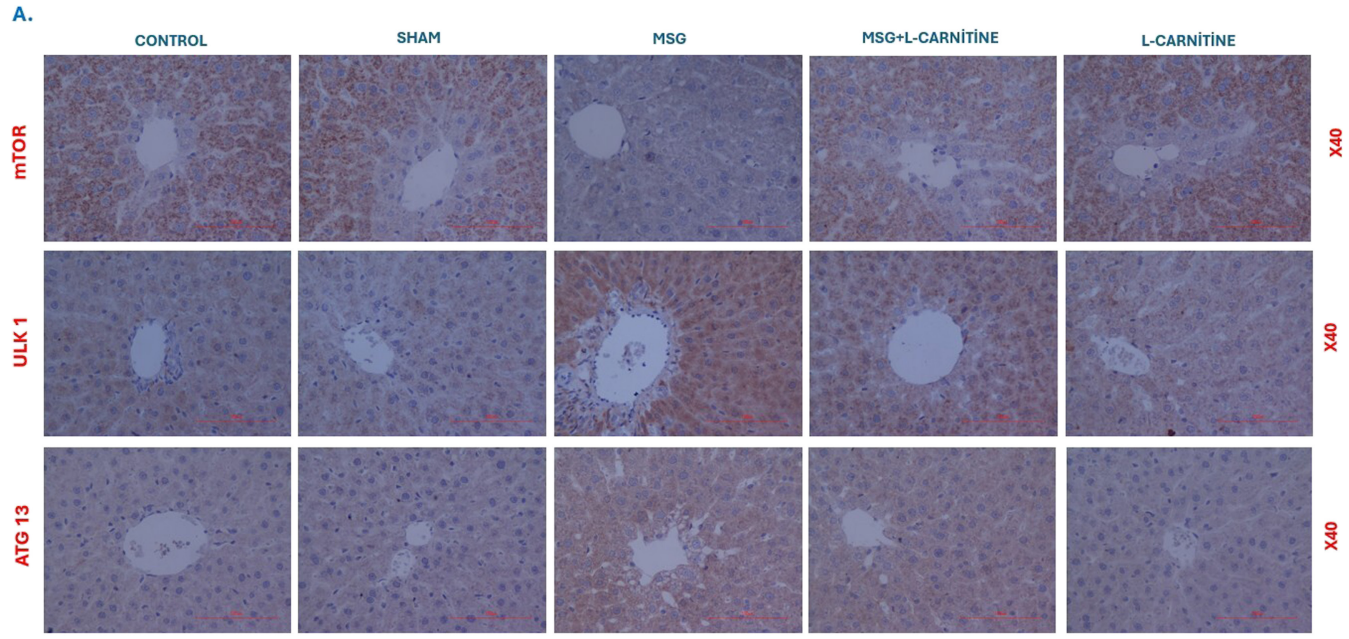

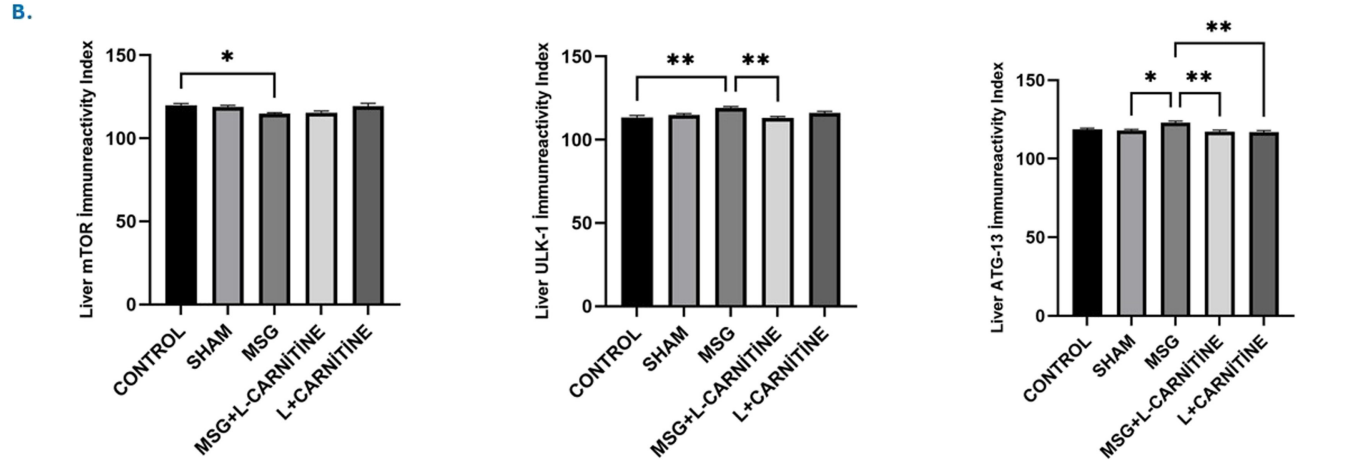

C.

İMMUNREACTİVİTY	CONTROL	SHAM	MSG	MSG+ L-CARNİTİNE	L-CARNİTİNE	P
mTOR	119.9 ± 2.728	118.9 ± 2.392	114.8 ± 1.762	115.4 ± 2.613	119.3 ± 4,638	.006
ULK-1	111.9 (110.0-118.8)	114.7 (110.3-118.4)	118.7 (116.8-123.2)	113.4 (108.3-116.5)	115.0 (111.8-120.6)	<.001
ATG-13	118.7 ± 2.600	117.8 ± 3.433	122.9 ± 3.950	117.1 ± 3.636	117.0 ± 3.448	<.001

FIGURE 4 | (A) Immunohistochemical light microscopic findings of autophagy-related indicators immunoreactivity in rat liver tissue of all groups. (Nikon Eclipse Si, Tokyo, Japan, 400×). Brown colored areas with DAB indicate positivity. (B) Graphical representation of autophagy-related indicators immunoreactivity in rat liver tissue groups. *$p < 0.05$, **$p < 0.01$, ***$p < 0.001$. Values are represented as mean ± SD using ANOVA and Kruskal–Wallis, followed as a post hoc Tukey test and Dunn's test, respectively. (C) Presentation of autophagy-related indicators immunoreactivity of liver tissue in different experimental groups in table form. Data were presented as mean ± standard deviation and median (min–max).

pattern comparable to that of the control group. In contrast, the MSG group displayed a significant reduction in mTOR staining intensity compared with the control group ($p < 0.05$). Although L-carnitine administration slightly increased mTOR immunoreactivity in the MSG + L-carnitine group, this change was not statistically significant ($p > 0.05$). The L-carnitine group alone demonstrated immunoreactivity levels similar to those observed in the control and sham groups (Figure 4B,C).

Immunoreactivity for ULK1 and ATG13 was detected in the periportal and perivascular regions as well as in the cytoplasm of hepatocytes. ULK1 expression was weak in the control, sham, and L-carnitine groups, whereas the MSG group exhibited a marked increase in ULK1 staining intensity (Figure 4A). Quantitatively, ULK1 immunoreactivity was significantly higher in the MSG group than in the control group ($p < 0.01$), and this elevation was significantly reduced following L-carnitine treatment ($p < 0.01$) (Figure 4B,C).

Similarly, ATG13 immunostaining was markedly elevated in the MSG group but remained low in the control, sham, and L-carnitine groups (Figure 4A). Compared with the sham ($p < 0.05$) and L-carnitine ($p < 0.01$) groups, the MSG group demonstrated a significant increase in ATG13 immunoreactivity, which was substantially attenuated after L-carnitine administration ($p < 0.01$) (Figure 4B,C).

3.4 | Serum AST and ALT Levels

The MSG group had greater serum AST levels than the control, sham, and L-carnitine groups, although the differences were not statistically significant ($p > 0.05$). This rise in the MSG group was lessened by L-carnitine treatment; however, this was not a significant improvement ($p > 0.05$) (Figure 5A,B).

When we looked at serum ALT levels, we found that the MSG group had higher levels than the control, sham, and L-carnitine groups. The MSG group exhibited an especially notable rise in comparison to the control group ($p < 0.05$). L-Carnitine therapy reduced the increase in serum ALT levels in the MSG group, but not significantly ($p > 0.05$) (Figure 5A,B).

4 | Discussion

MSG, a prevalent food additive, has been shown to cause hepatotoxicity, oxidative stress, and inflammatory responses in a variety of animals. Histopathological studies in liver tissue have revealed damage to the structure triggered by MSG, including cytoplasmic vacuolization, eosinophilia, sinusoidal dilatation, and fibrosis. Increases in proinflammatory cytokines (TNF-α and IL-1β) and autophagy-related markers (mTOR, ULK1, and ATG13) indicate that the damage is caused by both inflammatory and cellular processes. Serum AST and ALT levels increased in the MSG group, indicating hepatocellular damage, which was harmonious with histological and immunohistochemical findings. Together, these biochemical and morphological alterations point to an integrated pathogenic mechanism in which oxidative stress, inflammation, and impaired autophagy interact to drive hepatocellular injury.

In a mice study, MSG induced necrosis, pyknotic nuclei, mononuclear cell infiltration, congestion in the portal and central veins, and vacuolar degeneration in hepatocytes (El-Alfy et al. 2020). Shrestha et al. (2018) reported that MSG-treated rats exhibited central vein congestion and sinusoidal dilatation, whereas in the high-dose MSG group, endothelial rupture of the central vein and more pronounced hepatocellular damage were observed. In another study, Ahmed et al. (2019) showed that rats given MSG exhibited congestion

A.

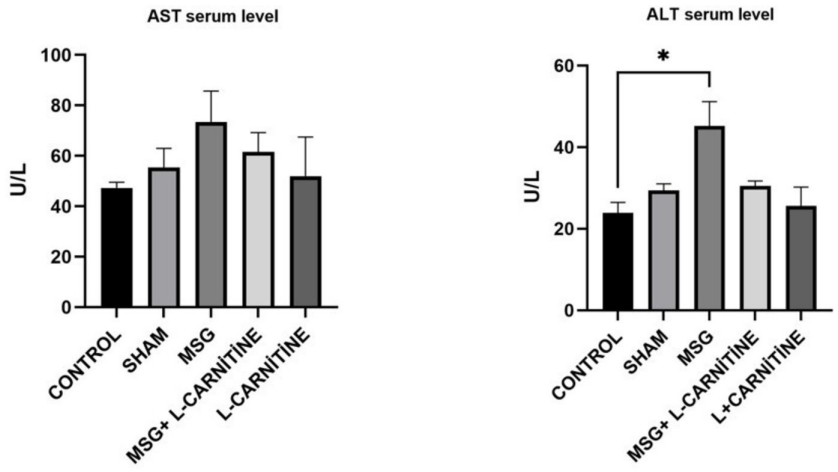

B.

SERUM LEVEL	CONTROL	SHAM	MSG	MSG+ L- CARNİTİNE	L-CARNİTİNE	P
AST	47.32 ± 4.473	55.34 ± 15.23	73.35 ± 24.74	61.58 ± 15.24	51.95 ± 30.97	.444
ALT	26.03 (16.10 - 27.30)	29.51 (25.64 - 32.99)	45.15 (30.62 - 59.78)	30.52 (28.14 – 32.89)	24.71 (15.83 -37.33)	.031

FIGURE 5 | (A) A statistical analysis of the experimental groups' serum levels of AST and ALT expressed graphically. Values are represented as mean ± SD using ANOVA and Kruskal–Wallis, followed as a post hoc Tukey test and Dunn's test, respectively. *$p < 0.05$, **$p < 0.01$, ***$p < 0.001$. (B) Presentation of AST and ALT levels of liver serum in different experimental groups in table form. Data were presented as mean ± standard deviation and median (min–max).

in the branches of the portal vein, inflammatory cell infiltration, proliferation of bile ductules, hepatocytes with pyknotic and karyolytic nuclei, severe vacuolization, dilated sinusoids, and central vein congestion. Neonatal MSG exposure induced long-term liver damage with disrupted cords, sinusoidal dilatation, and perivenous inflammation (Bhattacharya et al. 2011). Another study found that maternal MSG exposure during pregnancy caused structural liver damage in both mothers and fetuses (Gad El-Hak et al. 2021). A recent study demonstrated that MSG induces not only acute degenerative injury but also chronic histopathological alterations leading to fibrosis (Ezeuko et al. 2024). These findings, in conjunction with our results, reinforce the hypothesis that MSG exerts its hepatotoxic potential through persistent oxidative and inflammatory stress, culminating in structural remodeling and fibrosis.

Soliman et al. (2023) found that TNF-α and IL-1β levels ascended in serum after MSG-induced hepatotoxicity. Mashaal et al. (2025) showed that the MSG groups had considerably higher levels of TNF-α and IL-1β as well as increased liver inflammation. In our study, a marked increase in the immunoreactivity of inflammatory markers was detected as a result of MSG toxicity, with the elevation in IL-1β reactivity being particularly striking and fully consistent with the literature. In contrast, L-carnitine administration suppressed this increase in line with previous reports. This attenuation of inflammatory signaling suggests that L-carnitine's hepatorestorative effect may be partly mediated through the modulation of cytokine release and restoration of oxidative balance.

The interaction between MSG toxicity and autophagy is a relatively new area of research. MSG has been shown to impair autophagy in the testis and regulate the AMPK/mTOR pathway (Morsy et al. 2025). In contrast to our results, Araujo et al. (2019) reported that neonatal MSG exposure contributed to glucose intolerance and metabolic imbalances by disrupting insulin signaling through excessive activation of the mTOR pathway. Another study showed that MSG increased tsc1 expression in a fission yeast model, thus possibly affecting the mTOR pathway (Yılmazer and Kale 2025). ULK1 and ATG13 are important regulators of autophagy initiation. Under stress or damage, mTOR gets blocked, allowing ULK1 to phosphorylate and bind with ATG13, thereby starting autophagy (Puente et al. 2016; Rajak et al. 2022). Ganley et al. (2009) demonstrated autophagosome formation and ULK1–ATG13–FIP200 complex activity in culture experiments. Mao et al. (2023) confirmed that ULK1–ATG13 complex activity increased under stress and protected hepatocytes. In our study, MSG administration induced significant alterations in autophagy-related markers in liver tissue. A decrease in mTOR immunoreactivity was accompanied by increased ULK1 and ATG13 immunoreactivities. Although these variations were statistically significant, the magnitude of change was relatively small (3%–6%). This modest yet measurable shift likely represents a compensatory cellular adjustment rather than a full activation or suppression of autophagy. Even minor fluctuations in these critical regulators can substantially influence cellular homeostasis, particularly in metabolically active organs such as the liver. Therefore, these data suggest that MSG may subtly disturb the mTOR–ULK1–ATG13 signaling equilibrium, leading to cumulative cellular stress rather than overt pathway collapse. L-Carnitine treatment mitigated these alterations and restored marker levels toward baseline. Our results are consistent with previous evidence indicating that activation of the ULK1–ATG13 complex under stress protects hepatocytes, whereas mTOR inhibition promotes autophagy. Although the observed changes in autophagy-related markers were relatively modest in magnitude, they likely reflect a biologically meaningful adjustment rather than random variation, suggesting that MSG induces subtle modulation rather than complete suppression or activation of the autophagic pathway. Taken together, these observations imply that L-carnitine does not merely reverse MSG-induced damage but rather fine-tunes the autophagic process, allowing the cell to regain metabolic and structural stability. However, unlike studies reporting excessive mTOR activation following neonatal MSG exposure, our findings demonstrated suppressed mTOR activity in adult liver tissue. This discrepancy suggests that the biological effects of MSG may differ according to developmental stage, tissue specificity, and experimental conditions.

Banerjee et al. (2020) revealed that serum ALT and AST levels increased considerably in rats given a high-fat diet mixed with MSG. According to recent experimental research, MSG exposure significantly raises serum AST and ALT levels in rats (Moldovan et al. 2023; Maulina et al. 2024; Adikwu et al. 2025). Consistent with these findings, our study also demonstrated an elevation in both serum AST and ALT levels following MSG administration, with the increase in ALT levels being more pronounced. This further substantiates the hepatotoxic potential of MSG. The biochemical evidence of hepatic enzyme elevation aligns with the histopathological and immunohistochemical data, collectively supporting the conclusion that MSG triggers hepatocellular injury through oxidative and inflammatory mechanisms.

L-Carnitine is a natural substance that aids in energy metabolism and minimizes oxidative stress. It not only reduces inflammation but may also protect against toxic damage by regulating autophagic pathways (Khedr and Werida 2022). A study found that L-carnitine treatment for MSG-induced kidney injury minimizes inflammation and tubular degeneration while improving histology (Koohpeyma et al. 2021). Another study on aluminum chloride–induced liver damage found that simultaneous L-carnitine intake significantly repaired hepatocellular degeneration and inflammation (Alqhtani 2025). A high-fat diet-induced model showed that L-carnitine intake significantly decreased IL-1β, IL-6, and TNF-α levels (Sun et al. 2023). Biochemical assays also showed dose-dependent reductions in TNF-α and IL-1β in thioacetamide-induced liver fibrosis (Shalaby et al. 2024). In contrast to our findings, another study found that L-carnitine regulated autophagy by raising Beclin-1, ATG5, and ATG12 expression in testicular tissue (Khedr and Werida 2022). Another study demonstrated that L-carnitine autophagy indicators LC3 and P62 decreased in dexamethasone-induced steatohepatitis (Amer et al. 2024). This diversity in results suggests that the effects of L-carnitine on autophagy may be tissue specific and context dependent, possibly influenced by the type and severity of induced stress.

Our investigation found that MSG intake dramatically increased serum AST and ALT levels, which were significantly recovered with L-carnitine administration. This observation is consistent

with outcomes reported in the literature (Alqhtani 2025; Sun et al. 2023; Shalaby et al. 2024; Amer et al. 2024). Moreover, the contribution of our study lies in being the first to evaluate the regulatory effects of L-carnitine on autophagy-related markers in liver tissue. Our findings demonstrated that L-carnitine partially restored the reduction in mTOR immunoreactivity induced by MSG while attenuating the increases observed in ULK1 and ATG13, thereby normalizing marker levels toward those of the control group. This partial recovery further indicates that L-carnitine exerts its hepatorestorative action through multilevel regulation—by reducing oxidative and inflammatory burden while subtly rebalancing autophagic signaling to maintain cellular homeostasis. In this respect, our study differs from previous reports that examined autophagy markers in testicular or other organ models, and it fills an important gap in the literature regarding the regulation of autophagy in hepatic tissue.

Our study has certain limitations that should be acknowledged. Although histopathological, immunohistochemical, and biochemical analyses provided valuable information, molecular pathways and gene expression analyses that could further elucidate the underlying mechanisms were not performed. Although the regulatory effects of L-carnitine on autophagy-related markers were demonstrated, the evaluation was limited to mTOR, ULK1, and ATG13; other important markers such as Beclin-1, LC3, and p62, which could have further supported the study, were not examined. Moreover, the findings were obtained from an experimental rat model, and direct extrapolation to human physiology should be approached with caution. Future studies incorporating broader panels of autophagy markers and clinical validation will be essential to strengthen and extend our observations. Future studies focusing on time-dependent molecular responses and the inclusion of a wider spectrum of autophagy markers will be essential to fully delineate the dynamic interplay between MSG-induced injury and L-carnitine–mediated protection.

5 | Conclusion

In summary, this study demonstrates that neonatal exposure to MSG disrupts hepatic homeostasis through the combined activation of inflammatory and autophagic pathways, ultimately leading to structural and biochemical liver injury. The observed alterations in mTOR, ULK1, and ATG13 expression suggest that MSG induces a subtle imbalance in autophagic regulation rather than complete inhibition, thereby contributing to sustained cellular stress and hepatocellular dysfunction. L-Carnitine treatment effectively alleviated these changes by restoring autophagic equilibrium and reducing proinflammatory cytokine expression, indicating that its hepatorestorative action involves coordinated modulation of oxidative, inflammatory, and autophagic responses. These findings highlight L-carnitine's potential as a therapeutic candidate for mitigating xenobiotic-induced liver injury, particularly those associated with metabolic and autophagy-related disturbances. Nevertheless, future investigations employing molecular and gene expression analyses are warranted to confirm the mechanistic basis of these effects and to translate these findings into clinical relevance.

Author Contributions

Kubra Tuğce Kalkan: investigation, methodology, visualization, writing – original draft. **Ferhat Pektas:** conceptualization, methodology, investigation.

Acknowledgments

We would like to thank the individuals who took part in this study.

Funding

The authors have nothing to report.

Ethics Statement

The study was approved by the Animal Experiments Local Ethics Committee of the Kırşehir Ahi Evran University Animal Experiments Local Ethics Committee (Ethics Committee Decision No: 11/02, date: 27.05.2025). No human participants were involved in this study, and therefore, consent to participate is not applicable.

Consent

The authors have nothing to report.

Conflicts of Interest

The authors declare no conflicts of interest.

Data Availability Statement

The datasets used and analyzed during the current study are available from the corresponding author upon reasonable request.

References

Adeleke, D. A., A. O. Adewoyin, A. O. Ajayi, et al. 2022. "Effect of Monosodium Glutamate on the Body System." *World News Natural Science* 44: 1–23.

Adikwu, E., N. O. Ebong, and E. Julius. 2025. "Protective Effect of Silymarin on Monosodium Glutamate-Induced Liver Toxicity in Rats." *Biological and Biomedical Journal* 3: 62–69. https://doi.org/10.21608/bbj.2024.300220.1031.

Ahmed, R. R., M. Abdul-Hamid, S. R. Galaly, and H. M. Hamdalla. 2019. "Monosodium Glutamate-Induced Liver Microscopic and Biochemical Changes in Male Rats, and the Possible Amendment of Quercetin." *Egyptian Journal of Zoology* 71: 44–55. https://doi.org/10.21608/ejz.2019.37158.

Alqhtani, H. A. 2025. "Evaluation of L-Carnitine's Protective Properties Against AlCl3-Induced Brain, Liver, and Renal Toxicity in Rats." *PLoS ONE* 20: e0317939. https://doi.org/10.1371/journal.pone.0317939.

Amer, A. E., H. A. Ghoneim, R. R. Abdelaziz, G. S. Shehatou, and G. M. Suddek. 2024. "L-Carnitine Attenuates Autophagic Flux, Apoptosis, and Necroptosis in Rats With Dexamethasone-Induced Non-Alcoholic Steatohepatitis." *BMC Pharmacology and Toxicology* 25: 102. https://doi.org/10.1186/s40360-024-00820-z.

Araujo, T. R., J. A. da Silva, J. F. Vettorazzi, et al. 2019. "Glucose Intolerance in Monosodium Glutamate Obesity Is Linked to Hyperglucagonemia and Insulin Resistance in α Cells." *Journal of Cellular Physiology* 234: 7019–7031. https://doi.org/10.1002/jcp.27452.

Asejeje, F. O., G. O. Gabriel, and M. A. Abiola. 2023. "Monosodium Glutamate Aggravates Lipopolysaccharide-Induced Liver Injury via

Inflammation and Oxidative Stress in Rats." *Nutrire* 48: 5. https://doi.org/10.1186/s41110-023-00188-w.

Banerjee, A., D. Das, R. Paul, et al. 2020. "Mechanistic Study of Attenuation of Monosodium Glutamate Mixed High Lipid Diet Induced Systemic Damage in Rats by *Coccinia grandis*." *Scientific Reports* 10: 15443. https://doi.org/10.1038/s41598-020-72076-6.

Banerjee, A., S. Mukherjee, and B. K. Maji. 2021. "Monosodium Glutamate Causes Hepato-Cardiac Derangement in Male Rats." *Human & Experimental Toxicology* 40: S359–S369. https://doi.org/10.1177/09603271211049550.

Bayram, H. M., R. Uyar, R. Kocabaş, et al. 2023. "Monosodium Glutamate: Review on Preclinical and Clinical Reports." *Biointerface Research in Applied Chemistry*. https://doi.org/10.33263/BRIAC132.149.

Bhattacharya, T., A. Bhakta, and S. K. Ghosh. 2011. "Long Term Effect of Monosodium Glutamate in Liver of Albino Mice After Neonatal Exposure." *Nepal Medical College Journal* 13: 11–16.

Eid, R. A., M. Al-Shraim, M. S. Zaki, et al. 2019. "Vitamin E Protects Against Monosodium Glutamate-Induced Acute Liver Injury and Hepatocyte Ultrastructural Alterations in Rats." *Ultrastructural Pathology* 43: 199–208. https://doi.org/10.1080/01913123.2019.1673860.

El-Alfy, N. Z., M. F. Mahmoud, M. I. Eissa, and A. A. Emam. 2020. "Role of Propolis Against Toxic Effects of Monosodium Glutamate on Histology and Expression Lipid Metabolism Genes of Mice Liver." *Indian Journal of Public Health Research & Development* 11: 867–873. https://doi.org/10.37506/ijphrd.v11i5.9548.

Ezeuko, V. C., M. Omorose, S. M. Nweke, J. E. Aig-Unuigbe, and E. O. Imafidon. 2024. "Mitigating Potential of Ascorbic Acid Against Monosodium Glutamate-Induced Liver Fibrosis and Oxidative Stress in Wistar Rats." *Dutse Journal of Pure and Applied Sciences* 10: 116–125.

Gad El-Hak, H. N., H. M. Abdelrazek, D. W. Zeidan, A. A. Almallah, and H. E. Khaled. 2021. "Assessment of Changes in the Liver of Pregnant Female Rats and Their Fetuses Following Monosodium Glutamate Administration." *Environmental Science and Pollution Research* 28: 44432–44441. https://doi.org/10.1007/s11356-021-14649-2.

Ganley, I. G., D. H. Lam, J. Wang, X. Ding, S. Chen, and X. Jiang. 2009. "ULK1–ATG13–FIP200 Complex Mediates mTOR Signaling and Is Essential for Autophagy." *Journal of Biological Chemistry* 284: 12297–12305. https://doi.org/10.1074/jbc.M900573200.

García-Miguel, M., J. A. Riquelme, I. Norambuena-Soto, et al. 2018. "Autophagy Mediates Tumor Necrosis Factor-α-Induced Phenotype Switching in Vascular Smooth Muscle A7r5 Cell Line." *PLoS ONE* 13: e0197210. https://doi.org/10.1371/journal.pone.0197210.

Kasmara, D. P., Y. Prasetyo, D. R. Handayani, et al. 2025. "Mini Review of Plant Products as Food Supplement Against MSG-Induced Liver Injury: Antioxidant, Oxidative Stress and Histological Prospects." *Frontiers in Pharmacology* 16: 1522814. https://doi.org/10.3389/fphar.2025.1522814.

Kayode, O. T., J. A. Bello, J. A. Oguntola, A. A. A. Kayode, and D. K. Olukoya. 2023. "The Interplay Between Monosodium Glutamate (MSG) Consumption and Metabolic Disorders." *Heliyon* 9, no. 9: e19675. https://doi.org/10.1016/j.heliyon.2023.e19675.

Khedr, N. F., and R. H. Werida. 2022. "L-Carnitine Modulates Autophagy, Oxidative Stress and Inflammation in Trazodone Induced Testicular Toxicity." *Life Sciences* 290: 120025. https://doi.org/10.1016/j.lfs.2021.120025.

Koohpeyma, F., F. Gholizadeh, H. Hafezi, et al. 2022. "The Protective Effect of L-Carnitine on Testosterone Synthesis Pathway, and Spermatogenesis in Monosodium Glutamate-Induced Rats." *BMC Complementary Medicine and Therapies* 22: 269. https://doi.org/10.1186/s12906-022-03749-0.

Koohpeyma, F., M. Siri, S. Allahyari, M. Mahmoodi, F. Saki, and S. Dastghaib. 2021. "The Effects of L-Carnitine on Renal Function and Gene Expression of Caspase-9 and Bcl-2 in Monosodium Glutamate-Induced Rats." *BMC Nephrology* 22: 162. https://doi.org/10.1186/s12882-021-02364-4.

Lim, S. H., M. Hansen, and C. Kumsta. 2024. "Molecular Mechanisms of Autophagy Decline During Aging." *Cells* 13: 1364. https://doi.org/10.3390/cells13161364.

Mao, B., W. Yuan, F. Wu, Y. Yan, and B. Wang. 2023. "Autophagy in Hepatic Ischemia–Reperfusion Injury." *Cell Death Discovery* 9: 115. https://doi.org/10.1038/s41420-023-01341-8.

Mashaal, A., M. Mousa, H. T. Hamza, et al. 2025. "*Zingiber officinale* Mitigates Monosodium Glutamate-Induced Hepatic Pathology: Insights Into CD68-Macrophage Activation and Inflammatory/Apoptotic/Oxidative Mediators Crosstalk in Rats." *Journal of Taibah University for Science* 19: 2514286. https://doi.org/10.1080/16583655.2025.2514286.

Maulina, N., I. Zachreini, G. Gholib, A. Suwandi, and M. Akmal. 2024. "Black Garlic Exhibited Hepatoprotective Effect Against Monosodium Glutamate-Induced Hepatotoxicity in Animal Model." *Narra Journal* 4: e799. https://doi.org/10.52225/narraj.v4i2.799.

Moldovan, O. L., C. E. Vari, A. Tero-Vescan, et al. 2023. "Potential Defence Mechanisms Triggered by Monosodium Glutamate Sub-Chronic Consumption in Two-Year-Old Wistar Rats." *Nutrients* 15: 4436. https://doi.org/10.3390/nu15204436.

Morsy, M. M., H. A. Hassan, R. M. Morsi, O. E. Nafea, A. I. Farag, and R. S. Ramadan. 2025. "Alogliptin Attenuates Testicular Damage Induced by Monosodium Glutamate in Both Juvenile and Adult Male Rats by Activating Autophagy: ROS Dependent AMPK/mTOR." *Reproductive Toxicology* 132: 108826. https://doi.org/10.1016/j.reprotox.2025.108826.

Oluwole, D. T., O. S. Ebiwonjumi, L. O. Ajayi, et al. 2024. "Disruptive Consequences of Monosodium Glutamate on Male Reproductive Function: A Review." *Current Research in Toxicology* 6: 100148. https://doi.org/10.1016/j.crtox.2024.100148.

Puente, C., R. C. Hendrickson, and X. Jiang. 2016. "Nutrient-Regulated Phosphorylation of ATG13 Inhibits Starvation-Induced Autophagy." *Journal of Biological Chemistry* 291: 6026–6035. https://doi.org/10.1074/jbc.M115.702704.

Rajak, S., S. Raza, and R. A. Sinha. 2022. "ULK1 Signaling in the Liver: Autophagy Dependent and Independent Actions." *Frontiers in Cell and Development Biology* 10: 836021. https://doi.org/10.3389/fcell.2022.836021.

Ribas, G. S., C. R. Vargas, and M. Wajner. 2014. "L-Carnitine Supplementation as a Potential Antioxidant Therapy for Inherited Neurometabolic Disorders." *Gene* 533: 469–476. https://doi.org/10.1016/j.gene.2013.10.017.

Shalaby, M. A., A. Ramadan, S. S. Abd El-Rahman, and H. M. Fayed. 2024. "Hepatoprotective Effect of L-Carnitine Is Achieved via Activating Nrf2 and Targeting TLR4 Signaling Pathways in Thioacetamide-Induced Liver Fibrosis in Rats." *Life Sciences* 338: 122996. https://doi.org/10.36349/easjvms.2024.v06i03.002.

Shrestha, S., C. Jha, B. L. Das, and P. Yadav. 2018. "Effects of Monosodium Glutamate on Liver Tissue of Wistar Albino Rats – A Histological and Biochemical Study." *Experimental Animals* 8: 68–73. https://doi.org/10.3390/ani10111996.

Soliman, M. M., S. A. Althobaiti, and S. Sayed. 2023. "Ameliorative Impacts of *Rhodiola rosea* Against Hepatic Toxicity Induced by Monosodium Glutamate: Role of Inflammation-, Oxidative-Stress-, and Apoptosis-Associated Markers." *Journal of Taibah University for Science* 17: 2244749. https://doi.org/10.1080/16583655.2023.2244749.

Sun, C., Y. Guo, P. Cong, Y. Tian, and X. Gao. 2023. "Liver Lipidomics Analysis Revealed the Novel Ameliorative Mechanisms of L-Carnitine on High-Fat Diet-Induced NAFLD Mice." *Nutrients* 15: 1359. https://doi.org/10.3390/nu15061359.

Sun, Q., J. Fan, T. R. Billiar, and M. J. Scott. 2017. "Inflammasome and Autophagy Regulation: A Two-Way Street." *Molecular Medicine* 23: 188–195. https://doi.org/10.2119/molmed.2017.00077.

Virmani, M. A., and M. Cirulli. 2022. "The Role of L-Carnitine in Mitochondria, Prevention of Metabolic Inflexibility and Disease Initiation." *International Journal of Molecular Sciences* 23: 2717. https://doi.org/10.3390/ijms23052717.

Yılmazer, M., and D. Kale. 2025. "Monosodium Glutamate Induces tsc1 Gene Expression in Fission Yeast." *Frontiers in Life Science and Related Technologies* 6: 1–8. https://doi.org/10.3389/flsrt.2025.00001.

Zanfirescu, A., A. Ungurianu, A. M. Tsatsakis, et al. 2019. "A Review of the Alleged Health Hazards of Monosodium Glutamate." *Comprehensive Reviews in Food Science and Food Safety* 18: 1111–1134. https://doi.org/10.1111/1541-4337.12448.